Available online at www.sciencedirect.com
SCIENCE DIRECT®
Physics of the Earth and Planetary Interiors 143–144 (2004) 433–443
PHYSICS OF THE EARTH AND PLANETARY INTERIORS
www.elsevier.com/locate/pepi

The behaviour of sulphur in metal–silicate core segregation experiments under reducing conditions

Julien Siebert [a,b], Valérie Malavergne [a,*], François Guyot [b,c], Rossana Combes [a], Isabelle Martinez [d]

[a] *Laboratoire des Géomatériaux, Université de Marne-La-Vallée, Cité Descartes, Champs-sur-Marne, 77454 Marne-La-Vallée Cedex, France*
[b] *Institut de Physique du Globe de Paris, 4 Place Jussieu, 75 252 Paris Cedex 05, France*
[c] *Laboratoire de Minéralogie-Cristallographie, Case 115, 4 Place Jussieu, 75 252 Paris Cedex 05, France*
[d] *Laboratoire de Géochimie des Isotopes Stables, IPGP-Université Paris 7, 2 Place Jussieu, Tour 54-64, 75 252 Paris Cedex 05, France*

Received 17 December 2002; received in revised form 18 July 2003; accepted 29 July 2003

Abstract

Reactions between molten alloys and solid silicates were investigated under reducing conditions, down to four log units below the IW buffer, at 20–25 GPa and 2000 °C in the Mg–Si–Fe–O–S system. The iron-rich alloys formed in the Fe–Si–S ternary system were single phased at high-pressure and temperature, suggesting closure of the liquid immiscibility gap at these conditions. At the metal/silicate interface, the reduction of Fe^{2+} was coupled to oxidation of Si in metal, a reaction also observed in similar sulphur-free systems. Silicon and sulphur were observed to coexist simultaneously in the metal phase in contact with silicates and magnesium sulphide, MgS, was observed in the experiments. This latter phase would not segregate to the planetary cores, thus providing a reservoir of sulphur in the silicate and surficial planetary envelopes.

Keywords: Core segregation; Metal–silicate interactions; High-pressure and high-temperature experiments; Reducing conditions; Magnesium sulphide

1. Introduction

Metal/silicate interactions have been studied at pressures and temperatures corresponding to the transition zone and to the top of the lower mantle of the Earth by numerous authors (e.g., Ringwood and Hibberson, 1991; Ito et al., 1995; Othani et al., 1997; Li and Agee, 1996, 2001a,b; Righter et al., 1997; O'Neill et al., 1998; Gessmann et al., 2001; Wade and Wood, 2001). These conditions are considered pertinent in most models of Earth differentiation which imply a contribution of metal/silicate interactions at relatively moderate pressure and high-temperature conditions (e.g., Karato and Murthy, 1997). Moreover based on metal–silicate partition coefficients for siderophile elements obtained at high-pressure and high-temperature, several authors argue for an equilibrium between liquid metal and liquid silicate at the basis of a magma ocean at such pressure, temperature and oxygen fugacity conditions (e.g., Murthy, 1991; Li and Agee, 1996, 2001a; Othani et al., 1997; Righter et al., 1997; Walter et al., 2000; Drake, 2000). Understanding incorporation of silicon and sulphur in metal under these conditions is therefore important.

* Corresponding author. Tel.: +33-1-49-32-90-36; fax: +33-1-49-32-91-37.
E-mail address: malaverg@univ-mlv.fru.fr (V. Malavergne).

0031-9201/$ – see front matter © 2004 Elsevier B.V. All rights reserved.
doi:10.1016/j.pepi.2003.07.022

Some geochemical mass balance calculations imply core models with significant Si amounts (MacDonald and Knopoff, 1958; Allègre et al., 1995, 2001; Javoy, 1995). It should be noticed that the missing Si could be also sequestred in a lower mantle chemically different from the upper mantle (Anderson, 1988; Javoy, 1995) or could be due to Earth accreting materials with a super-chondritic Mg/Si ratio. In this study, we investigate the first possibility, that is the presence of significant amounts of Si in metal which is not immediately consistent with the average oxygen fugacity of the Earth as deduced from the bulk Fe^{2+} content in the upper mantle. Reductive incorporation of Si in metal could explain the coexistence of a silicon-rich core with a Fe^{2+}-rich mantle according to:

$$SiO_{2\,\text{in silicates}} + 2Fe_{\text{in metal}} \leftrightarrow 2FeO_{\text{in silicates}} + Si_{\text{in metal}} \quad (1)$$

Several authors have studied process (1) for pressures ranging between ambient values to 27 GPa and at high temperatures (Ito et al., 1995; Guyot et al., 1997; Othani et al., 1997; O'Neill et al., 1998; Gessmann et al., 1999, 2001; Li and Agee, 2001a,b; Malavergne et al., 2004). Only few have investigated the role of sulphur on process (1) (Kilburn and Wood, 1997; Li and Agee, 2001a,b). Sulphur is a major element present in metal phases of all metal-bearing chondrite groups. It has been proposed as an important element in the core of the Earth (Murthy and Hall, 1970; Walker et al., 1993; Li and Agee, 1996, 2001a,b; Othani et al., 1997). However, liquid immiscibility in the Fe–Si–S system at ambient pressure (Raghavan, 1988; Poirier, 1994) and possibly at higher pressure, as well as difficulties for incorporating simultaneously Si and S in metal (Kilburn and Wood, 1997), have led to discussions about its abundance in the Earth's core. Moreover, geochemical constraints based on elemental volatilities suggest a maximum abundance of 1–2 wt.% of S in the core (Dreibus and Palme, 1996; Allègre et al., 2001). Keeping in mind current uncertainties on core formation models, as well as the large diversity of possible scenarios, it is still of interest, however, for planetary differentiation studies, to determine how sulphur behaves in the presence of Si-bearing metal, i.e., how it may interact with process (1).

The purpose of this study has thus been to carry out (Fe–Si–S) alloy/silicate core segregation experiments. The main goal was to determine the reactivity of simultaneously Si and S rich metals (possibly biphasic) with silicates in order to compare with results obtained on Fe–S–silicate systems under more usual less reducing conditions (Walker et al., 1993; Othani et al., 1997; Li and Agee, 1996, 2001b).

2. Experimental procedure

The starting materials used were FeS (Goodfellow^{TM}, 99.9% pure), Si (Goodfellow^{TM}, 99.9% pure), natural enstatite $(Mg_{0.88}Fe_{0.12})SiO_3$ from San Carlos (Arizona, USA), hereafter labelled SC enstatite, containing 1 wt.% of Ca and 4.8 wt.% of Al, synthetic enstatite ($MgSiO_3$). Synthetic enstatite was synthesised according to procedure given by Thiéblaut et al. (1999). Fine-grained powders of FeS, Fe and Si, typically 15–20 μm, were intimately mixed and used as the metallic component. The dried materials were grounded together in appropriate proportions in an agate mortar in pure alcohol. Compositions and proportions of starting materials used in the different runs are given in Table 1.

High-pressure and high-temperature experiments were performed using a 1200 t multianvil apparatus at the Bayerisches Geoinstitut, Germany. The pressure assembly consisted of Cr-doped MgO octahedron with an edge length of 14 or 10 mm in the pressure range of 10–25 GPa. The octahedron was compressed using 32 mm carbide anvils with truncation edge length of 8 or 4 mm, with 14 and 10 mm octahedra, respectively. The samples were contained either in polycrystalline MgO or in single crystal MgO capsules. The capsule was surrounded by cylindrical resistance heater of $LaCrO_3$. The description of the cell assembly is shown in Fig. 1. Using single crystals of MgO has proven useful for reducing leakage of the low viscosity material contained in the samples at high pressures and temperatures as well as for minimising reactions between samples and capsules. Temperatures were measured with a W3%Re–W25%Re thermocouple inserted coaxially with thermocouple junction in contact with one hand of the sample capsule. Pressure calibrations for these assemblies are given by Rubie (1999). The *P–T* uncertainties are estimated to be ±1 GPa and ±100 K, respectively. In each experiment, the sample was first compressed to the desired

Table 1
Experimental runs and starting material compositions

Runs	S2852[a]	S2853[b]	S2861[b]	BT14[c]
Capsule	MgO single crystal	MgO single crystal	MgO single crystal	MgO polycrystal
Pressure, P (GPa)	20	20	25	14
Temperature, T (°C)	2000	2000	2000	1700
Duration (min)	10	10	9	45
Starting metal composition (at.%)				
Fe	35.96	24.82	24.82	83.85
S	35.96	24.82	24.82	16.15
Si	28.08	50.36	50.36	0
Starting metal composition (wt.%)				
Fe	50.80	38.45	38.45	90
S	29.20	22.10	22.10	10
Si	20.00	39.45	39.45	0

[a] Starting mixes are as follows: 4 wt.% Si metal, 16 wt.% FeS, 80 wt.% SC enstatite $(Mg_{0.88}Fe_{0.12})SiO_3$.
[b] Starting mixes are as follows: 7.5 wt.% Si metal, 11.5 wt.% FeS, 81 wt.% SC enstatite $(Mg_{0.88}Fe_{0.12})SiO_3$.
[c] Starting mixes are as follows: 33 wt.% $Fe_{0.9}S_{0.1}$, 67 wt.% synthetic enstatite ($MgSiO_3$).

pressure and then heated to the desired temperature at a rate of 200 °C/min. The samples were quenched by switching off the electrical power. The quench rate was approximately 500 °C/s. After quenching, samples were decompressed over 12 h. The entire sample plus pressure assemblies were then mounted in epoxy, sectioned through their centers, and their surfaces were polished and eventually carbon coated for scanning electron microscopy (SEM) analyses.

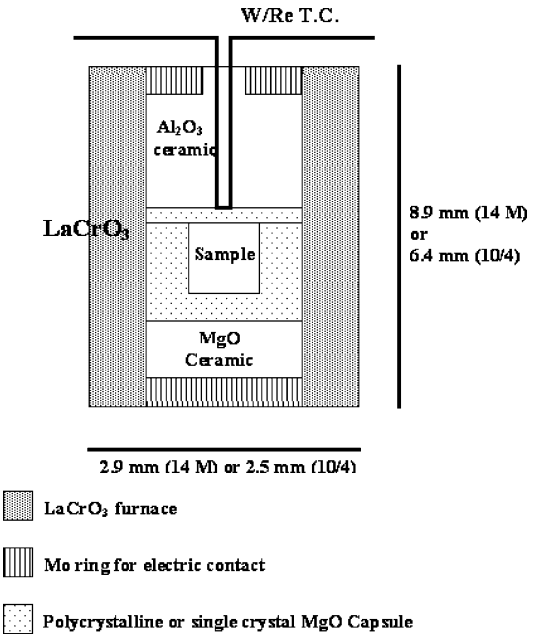

Fig. 1. Schematic drawing of the cell assemblies used in these experiments.

Samples were studied and analysed by optical microscopy, by SEM (Leo™ Steroscan 440) equipped with a Princeton™ Gamma-Tech PGT™ Spirit energy-dispersive X-ray analyser (EDX) able to analyse oxygen quantitatively, and Raman spectroscopy (XY Dilor™). Operating conditions of the SEM were an accelerating voltage of 20 kV; counting times were of about 100 s with a beam current of 0.5 nA for each EDX analysis and of 1 s per point with a beam current of 2 nA for quantitative chemical maps. Standards used were pure Fe metal and FeS for Fe and S, wollastonite or quartz and FeSi for Si, MgO for Mg, wollastonite for Ca and Al_2O_3 for Al. Raman spectra were recorded between 200 and 1400 cm^{-1} with acquisition times between 120 and 600 s and with an incident laser power between 10 and 100 mW. The argon laser beam tuned at 514 nm, was focused through microscope objectives (×100) down to approximately 1 μm.

3. Experimental results

In the three samples initially containing distinct grains of FeS and Si (samples S2852, S2853, S2861), these two phases, well separated prior to the runs, have

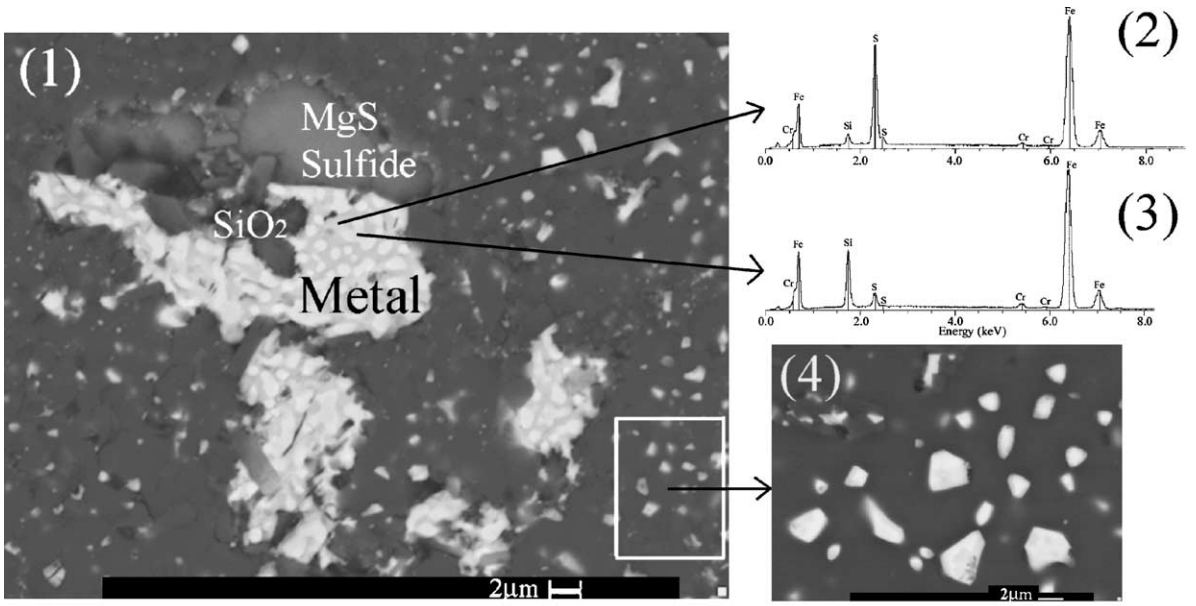

Fig. 2. (a) Backscattered electron image of sample S2861 (25 GPa) showing Fe–S rich, Si-poor phase (light grey and EDX spectrum) and Fe–Si rich, S poor phase (white and EDX spectrum). SiO_2 and MgS-sulphide are observed in contact with metal. An enlargement of the region enclosed by the white frame shows a detail of small metal particles formed by reduction of majorite. The metallic particles also contain two different contrasts corresponding to Fe–Si rich, S poor phase (white) and Fe–S rich, Si-poor phase (light grey). (b) Backscattered electron image of sample S2853 (20 GPa) showing similar phases as in 25 GPa samples. The magnesium sulphide phase has a stoichiometry close to MgS (EDX spectrum) and contains little amounts of Ca and Fe. Rods of SiO_2 stishovite, biphasic quenched metal phase and tiny biphasic metal particles are visible.

Table 2
Analyses of metal and silicates phases in sulphur bearing samples

Runs	S2852	S2853	S2861
Capsule	MgO single crystal	MgO single crystal	MgO single crystal
P (GPa)	20	20	25
T (°C)	2000	2000	2000
Duration (min)	10	10	9
ΔIW	−2.8	−3.6	−3.8
Metal liquid composition (wt.%)[a]			
Fe	66.3	63.5	61.6
S	29.1	17.0	17.7
Si	4.6	19.5	20.7
Metal liquid composition (wt.%)[b]			
Number of analyses	13	14	14
Fe	65.3 (1.0)	63.0 (3.6)	62.2 (1.0)
S	30.5 (2.3)	17.5 (3.9)	18.4 (1.2)
Si	4.2 (1.2)	19.5 (5.6)	19.4 (1.6)
Silicate composition in oxide (wt.%)			
Number of analyses	10	10	10
SiO_2	56.0 (1.2)	58.1 (0.9)	58.2 (0.6)
MgO	37.4 (0.9)	35.9 (0.7)	36.0 (0.6)
Al_2O_3	4.3 (0.2)	4.7 (0.1)	4.9 (0.1)
CaO	0.9 (0.05)	1.0 (0.05)	1.1 (0.05)
FeO	1.4 (0.1)	0.5 (0.03)	0.4 (0.03)

Numbers in parentheses are the standard deviations. Silicate was analysed for Fe, Si, Mg, S, Ca and Al. No significant amount of S was detected (less than 0.1 wt.%). ΔIW: oxygen fugacity relative to the iron-wüstite buffer based on the Fe–FeO equilibrium; for details see text.

[a] Metal composition reintegrated on the basis of the chemical maps (see text).

[b] Metal composition estimated by using a window size just smaller than the size of the metal blobs. Metal was analysed for Fe, Si, S. The presence of few amounts of Cr in a few metal blobs (<1 wt.%) is not shown. No significant oxygen was detected in the metal. However, the presence of small amounts of oxygen (<1 wt.%) in the metal cannot be ruled out.

coalesced into single large metallic blobs (Fig. 2). SEM images reveal that this metal contains two phases: an Fe–S rich, Si-poor phase and an Fe–Si rich, S poor phase (Fig. 2). The small dimensions of these two intergrown phases (typically less than 1 μm) do not allow single phase microanalysis with the EDX system of the SEM, even using a focused beam. In order to obtain analyses of the bulk metal phase, we used a window of size just smaller than the size of the metal particles (Table 2). The large standard deviation reflects some scatter in the analyses due to the non-negligible size of the two intergrown phases constituting the metal blobs, with regard to the window size, typically between 10 and 100 μm^2. In an alternative method, representative areas in each sample were selected and chemically mapped (around 7500 analyses for the metal phase in each map) by quantitative chemical mapping. Average element concentrations in the metal were then obtained (Table 2) by recombining the analyses using the SPIRIT-image analysis software.

The silicate material is mostly majorite, as revealed by its composition (Table 2) and Raman spectra (Fig. 3). It contains tiny metallic droplets, well visible in Fig. 2, which make the quantitative determination of the iron content in majorite difficult. However, some rare areas in majorite are free of metal droplets at the scale of the SEM observations, which allows obtaining the iron content in this phase. With these values, it is possible to estimate the effective oxygen fugacities that have prevailed during the experiments, relative to the iron-wüstite (IW) equilibrium according to the following equation:

$$\log fO_{2\,\text{experiment}} = \log fO_{2\,\text{IW}} + 2\log\left(\frac{a_{\text{FeO}}}{a_{\text{Fe}}}\right) \quad (2)$$

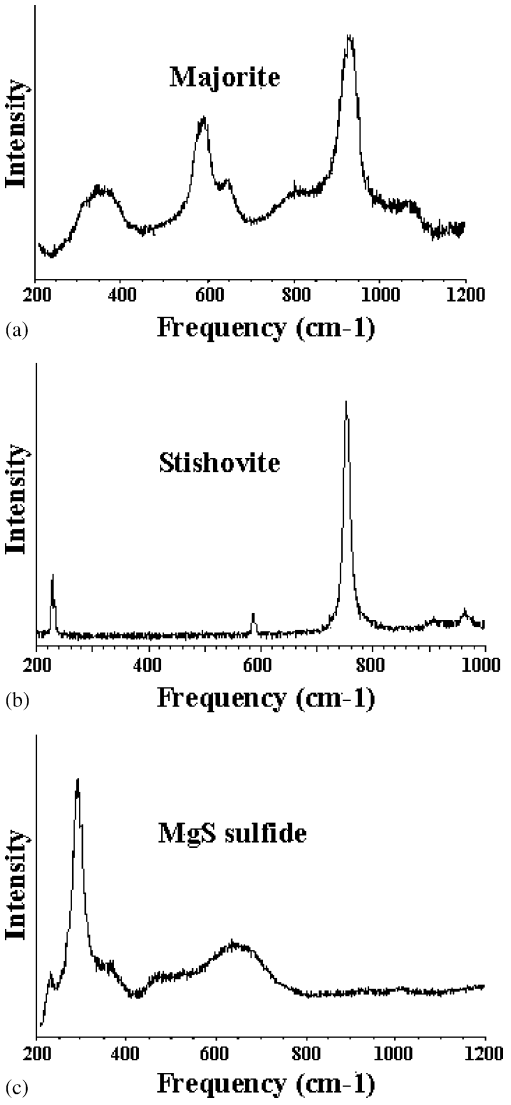

Fig. 3. (a) Raman spectrum of silicate in sample S2861. This spectrum is in good agreement with the spectrum of majorite obtained by Rauch et al. (1996). (b) Raman spectrum of the SiO_2 phase in sample 2861. This spectrum is in good agreement with the spectrum of stishovite obtained by Gillet et al. (1990). (c) Raman spectrum of the MgS-sulphide phase in sample 2861. Notice that MgS niningerite has no first order Raman spectrum.

where a_{FeO} and a_{Fe} are respectively the activities of FeO in silicate and Fe in liquid metal. In the absence of magnesiowüstite in the samples, due to lack of reactions between the MgO single crystalline capsule and the samples, fO_2 must be estimated by using the majorite-metal equilibrium. Unfortunately, the poor knowledge of activity-composition relations in majorites does not allow to easily retrieve oxygen fugacities. It is however possible to calculate the equilibrium a_{FeO} in magnesiowüstite by combining our analytical data in majorite with measurements from previous works about Fe partitioning between magnesiowüstite and majorite at relevant conditions (Tronnes, 2000; Wood, 2000; Frost, 2003). It appears that the most recent determinations (Frost, 2003) show that the partition coefficient between magnesiowüstite and majorite is close to unity at low total Fe contents. This behaviour has been observed with other silicates as well (Frost et al., 2001; Frost, 2003). At the low FeO contents of the present experiments, the activities of FeO can thus be considered to be close in magnesiowüstite and majorite. Taking into account non-ideality in magnesiowüstite (Fei et al., 1991) would lead to a maximum correction of 0.6 log units in oxygen fugacity, in agreement with previous estimates (Gessmann et al., 1999). Since this difference is not large and keeping in mind the large uncertainties which remain about activity-composition relations at high-pressure, results using a partition coefficient of 1 between majorite

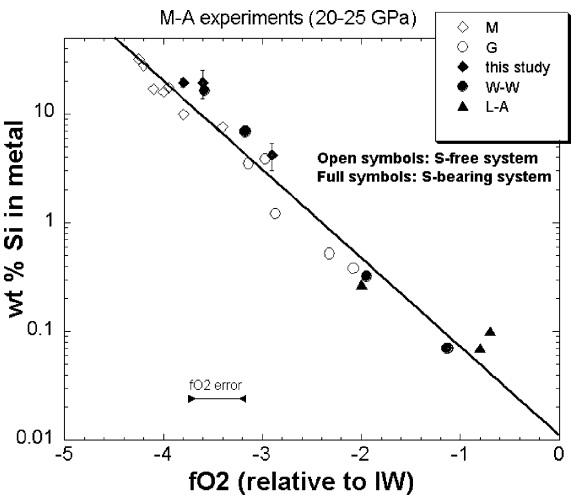

Fig. 4. wt.% Si in the metallic phase as a function of $\log fO_2$ for this study and previous studies at similar conditions. Oxygen fugacities are given relative to the IW buffer using FeO content in metal and liquid silicates (W–W, L–A) or solids (M, G, this study). Open symbols: S-free experiments. Data from M: Malavergne et al., 2004; G: Gessmann et al., 2001. Filled symbols: S-bearing experiments. Data from this study, W–W: Wade and Wood, 2001; L–A: Li and Agee, 2001b.

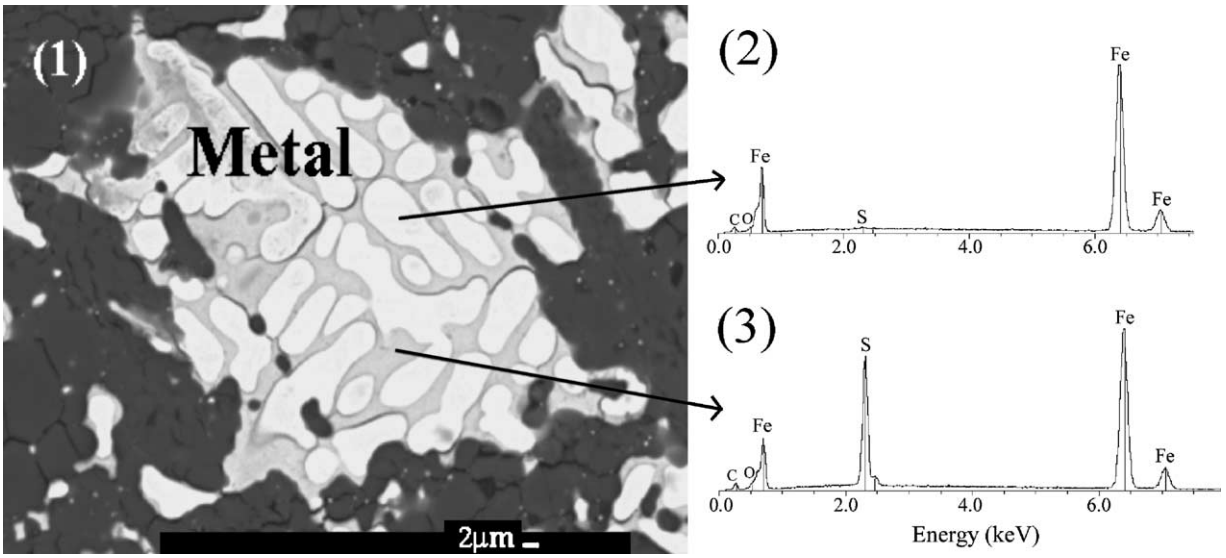

Fig. 5. Backscattered electron image of sample BT14 showing the quenched liquid metal containing two phases: Fe–S poor liquid (white and EDX spectrum) and Fe–S rich liquid (light grey and EDX spectrum). Neither stishovite nor magnesium sulphide have been evidenced in this sample.

and magnesiowüstite and an ideal model in magnesiowüstite are reported in Fig. 4, consistently with the approach of Gessmann et al. (1999).

A SiO_2 phase identified as stishovite by Raman spectroscopy (Fig. 3) is observed at the contact between the metal and majorite phases. At the contact with the metal phase, a phase of MgS composition containing minor amounts of Fe and Ca, is also observed (Fig. 2). The Raman spectrum of this phase is shown in Fig. 3; the assignment of the observed modes to a structure is not straightforward. Cubic monosulphides (space group *Fm*3*m*) have no first order Raman spectra. This magnesium sulphide phase is thus likely a high-pressure polymorph of MgS, the structure of which awaits to be determined.

Finally, a sample consisting of a starting assemblage of Fe, FeS and synthetic enstatite was transformed at 14 GPa and 1700 °C (sample BT14, Table 1). Even if the run conditions are quite different, this sample provided a useful reference for the reactivity of a similar system in the absence of reduced silicon. In this sample, the initially well separated Fe and FeS phases have coalesced into single metallic blobs, which contain two phases in the quenched samples (Fig. 5). These two phases are a Fe-rich, S poor phase and a Fe-sulphide phase close to Fe_2S in stoichiometry. Neither MgS nor stishovite have been evidenced in this sample. This Fe–S–silicates was previously studied in literature (Walker et al., 1993; Othani et al., 1997; Li and Agee, 1996, 2001a,b; Holzheid and Grove, 2002). No formation of MgS is reported from these studies.

4. Discussion

4.1. Fe–Si–S ternary system

In both Si-containing and Si-free experiments, the observed metal blobs are well segregated into one single phase after reaction at high-pressure and high-temperature, although in the starting material two different metal phases were present in each sample: Fe and FeS in the Si-free system and FeS and Si in the Si-bearing system. These metal particles are constituted by two distinct intergrown phases after quench and pressure release. These two intergrown phases are always in close association in the whole samples. This is strong evidence that the liquid metal was a single phase at high-pressure and temperature. This result has long been established in the Fe–S system; it was not obvious in the Fe–S–Si system due to the existence of a liquid immiscibility gap at

1 bar (e.g., Raghavan, 1988 for Fe–S and Fe–S–Si phase diagrams). Our observations thus suggest that, at 2000 °C and 20–25 GPa, the immiscibility gap is closed in the Fe–S–Si system, or at least considerably reduced, since our metal composition would fall well within the gap existing at 1 bar. Moreover, the sizes of the two intergrown phases within metal blobs in the four samples investigated (typically less than 1 μm) are consistent with textures developing during quench. This result is consistent with recent observations by Sanloup and Fei (2004) who observed the presence of a single metallic liquid (Fe–18 wt.% S–8.5 wt.% Si) liquid at 20 GPa and −1900 °C. It is also consistent with the report of a metal phase with 16.4 wt.% of Si and 3.5 wt.% of S at 2300 °C and 25 GPa by Wade and Wood (2001). The argument of immiscibility in the Fe–S–Si system thus cannot be used for excluding simultaneous presence of Si and S in the Earth's core.

In the three samples investigated in the Fe–S–Si metal system, some silicon was oxidised to stishovite. Abundant metal droplets are observed within the silicate phase showing that Fe^{2+} in majorite was reduced (e.g., Fig. 2). These two processes are coupled by oxygen balance as:

$$2FeSiO_{3\,\text{in silicate}} + Si_{\text{metal}} \leftrightarrow 3SiO_2 + 2Fe_{\text{metal}} \quad (3)$$

The Si content in metal (Table 2) is not very different from that measured in a sulphur-free system at the same conditions (Fig. 4, Table 3). Table 3 shows that the presence of sulphur in metal does not drastically affect the final composition for similar reduction states of the starting materials. Therefore, under the conditions investigated, sulphur does not appear to have a strong effect on process (1) or (3). Liu and Fleet (2001) have shown that, at 1 bar and 1000–1400 °C, sulphur has a strong effect on the partition coefficient of Si between solid and liquid metal, changing from 0.45 in S-free systems to 3 for S contents relevant to our experiments. If all this effect was due to S–Si interactions in liquid metal, this should decrease the Si content of our S-bearing experiments by about 10% in comparison with S-free systems. Such a difference is too close to the analytical error on Si determination in metal (Table 3) to allow discussion of this effect. The results also show that, at least in some cases, silicon and sulphur can be present simultaneously in large quantities in a metal phase in contact with silicates. This result might appear contradictory with reports from experiments at lower pressures (2.5 GPa and −2000 °C) by Kilburn and Wood (1997) that would exclude simultaneous presence of silicon and sulphur in the metal phase. Insufficient reaction times which would lead to underestimated silicon or sulphur extraction in our experiments are not likely for two reasons: first, no compositional gradients are observed in the silicate matrix; second, small metal droplets formed by reduction of majorite contain Si and S which would be impossible if the equilibrium composition was fully depleted in one of the two elements. The observed coexistence of Si and S in metal could be due to the absence of an S-bearing silicate melt at 2000 °C in our experiments. In the absence of a melt, the activity of sulphide ions in the non-metal phase would be presumably larger, thus explaining larger S contents in metal. However, experiments by Wade and Wood (2001) at 20 GPa and 2300 °C seem to indicate Fe–Si–S metals even in the

Table 3
Comparison of Si contents (wt.%) in metal in sulphur-free and sulphur bearing metal/silicate experiments under highly reducing conditions

	S2852	S2853	S2861	2860[a]	2561[b]	2416[c]
P (GPa)	20	20	25	20	20	25
T (°C)	2000	2000	2000	2000	2200	2000
Duration (min)	10	10	9	1	7	60
Si/O[d] (wt.%)	0.59	0.79	0.79	0.65	0.72	0.68
Si (wt.%)[e]	4.2 (1.2)	19.5 (5.6)	19.4 (1.6)	7.60 (0.07)	17.60 (0.12)	16.00 (0.09)

[a] Starting mixes are as follows: 85 wt.% SC enstatite, 15 wt.% $Fe_{0.83}Si_{0.17}$ (Malavergne et al., 2004).
[b] Starting mixes are as follows: 85 wt.% SC enstatite, 15 wt.% FeSi (Malavergne et al., 2004).
[c] Starting mixes are as follows: 80 wt.% SC enstatite, 20 wt.% FeSi (Malavergne et al., 2004).
[d] Si/O in starting material. This ratio is an indicator of the reduction state of the sample (e.g. Gessmann et al., 1999).
[e] Uncertainties on Si determination in metal are given in parentheses. The large uncertainty on the determinations of the present study is due to the biphasic nature of the quenched metal phase.

presence of a melt. Alternatively, a pressure effect on chemical equilibria could explain differences between samples at 2.5 GPa (Kilburn and Wood, 1997) and at 20–25 GPa (Wade and Wood, 2001, and this study). Further experiments at intermediate pressures are needed to elucidate this issue. In any case, the simultaneous presence of Si and S in an Fe-alloy equilibrated with silicates cannot be ruled out under some plausible primitive Earth differentiation conditions.

4.2. MgS formation in reducing segregation

In the three samples investigated in the Fe–S–Si metal system, a magnesium sulphide (MgS) was formed at the rim of metal particles, whereas it was systematically absent in Si-free experiments. Cubic monosulphide series with the general formula (Mg,Mn,Ca,Fe)S are common phases in enstatite chondrites and in some achondrites (see Keil, 1989, for a review and extensive references). The formation of these sulphides requires exceptionally low oxygen and high sulphur fugacities (e.g., Larimer and Bartholomay, 1979). In our experiments, the formation of MgS through:

$$FeS_{\text{in metal}} + MgSiO_{3\,\text{in silicate}} \leftrightarrow MgS + FeSiO_{3\,\text{in silicate}} \quad (4)$$

is possible only under highly reducing (below IW-3) conditions at which it can be coupled to reaction (3). The sum reaction is then written as:

$$2FeS + 2MgSiO_3 + Si_{\text{in metal}} \leftrightarrow 2MgS + 3SiO_2 + 2Fe_{\text{in metal}} \quad (5)$$

Our results mean that reaction (5) is proceeding toward formation of MgS at 20–25 GPa and 2000–2200 °C. It is worth emphasising that, at 1 bar and 300 K, thermodynamic data ($\Delta_r G^\circ \sim -104$ kJ, Chase, 1998) suggest that MgS formation would occur as long as activity of Si in the metal phase is large enough. Carbon has been proposed as a reducing agent for MgS formation (Fleet and Mac Rae, 1987), although it might be insufficiently reducing (Larimer and Ganaparthy, 1987). Even at low pressure, Si in metal could be an alternative reducing agent efficient for magnesium and calcium sulphidation.

Magnesium sulphide, MgS, is a low density material (2.7 at 1 bar and 300 K). Using results from diffraction experiments on MgS at high-pressure by Peiris et al. (1994) and a third-order Birch–Murnaghan equation of state yields a density of 3.2 at 20–25 GPa and room temperature. Even if the MgS phase observed in our experiments is indeed a denser high-pressure polymorph, as suggested by the Raman spectra, MgS as a separate phase will remain a low density phase in comparison with metal. Therefore, this sulphur bearing phase would not segregate to the core with metal phases. If the core segregation in the Earth or in planetesimals implied Si-bearing liquid metal percolating through sub-solidus silicates, Mg–Ca sulphides would constitute a major form of sulphur sequestred in the silicate part of the planet. This would be an additional mechanism to fractionate Mg/Si in the early Earth. MgS is an highly refractory phase, however quite unstable in the presence of water. Further mixing of MgS buoyantly segregated to the shallow mantle with more oxidised hydrated components (Wänke and Dreibus, 1988), could then destabilise this phase according to:

$$MgS + H_2O \leftrightarrow MgO + H_2S \quad (6)$$

which could have delivered significant quantities of H_2S to the surface of the primitive Earth. It should be noticed, however, that numerous metal/silicate segregation models of the Earth, but not of planetesimals, imply molten instead of sub-solidus silicates. Recent experiments about the melting behaviour of enstatite chondrites (McCoy et al., 1999; Fogel, 1998; Dickinson et al., 1998) indicate that at temperatures exceeding 1300 °C at 1 bar, sulphides dissolve into an S-rich silicate melt. The consequences for sulphur behaviour could then be very different since no separate (Mg,Ca)S phase would form. We note however that Ca,Mg,Mn monosulphides have been reported to form by fractional crystallisation from S-bearing silicate melts under highly reducing conditions (McCoy et al., 1999). (Mg,Ca)S sulphides might thus be important phases even in differentiation processes involving partially or totally molten silicates.

5. Conclusion

We have performed core segregation experiments at 20–25 GPa and 2000 °C, using assemblages of

sub-solidus silicates and (Fe–Si–S) metal alloys. Our observations suggest that, at these pressures and temperatures, the immiscibility gap in the ternary Fe–S–Si system is closed. The argument of immiscibility in the Fe–S–Si system thus cannot be used for excluding simultaneous presence of Si and S in planetary cores. Moreover, we show that appropriate P–T–fO_2 conditions exist under which silicon and sulphur can be present simultaneously in a metal phase in contact with silicates. This is a different conclusion than in previous studies and could be due to the absence of S-bearing silicate melts in our experiments. The simultaneous presence of Si and S in an Fe-alloy equilibrated with silicates thus cannot be ruled out under some plausible Earth or planetesimals differentiation conditions. Finally, magnesium sulphide, MgS, a low density material was formed in the experiments. If the core segregation in the Earth or in planetesimals implied Si-bearing liquid metal percolating through sub-solidus silicates, Mg–Ca sulphides would then have constituted a reservoir of sulphur in the silicate part of the planet, which upon hydration could have delivered significant quantities of H_2S to the early planetary surfaces.

Acknowledgements

High-pressure and high-temperature experiments were performed at Bayerisches Geoinstitut, Germany, under the EU "IHP-Access to Research Infrastructures" Programme (contract no. HPRI-1999-CT-00004 to D.C. Rubie). We thank Dan Frost and Stephan Borensztajn for respective assistance with multianvil experiments and SEM observations. The French INSU-CNRS Programs PNP, Planétologie, and Terre Profonde are thanked for financial support. We wish to thank C.B. Agee and K. Righter for their constructive and insightful reviews.

References

Allègre, C., Poirier, J.P., Humler, E., Hofman, A., 1995. The chemical composition of the earth. Earth Planet. Sci. Lett. 134, 515–526.

Allègre, C., Manhès, G., Lewin, E., 2001. Chemical composition of the earth and the volatility control on planetary genetics. Earth Planet. Sci. Lett. 185, 49–69.

Anderson, D.L., 1988. Composition of the earth. Science 243, 367–370.

Chase, M.W. Jr., 1998. NIST-JANAF thermochemical tables, 4th ed. J. Phys. Chem. Ref. Data, Monograph 9, 1–1951.

Dickinson, T.L., McCoy, T.J., Lofgren, G.E., 1998. Melting of indarch (EH4) powders: phase relations and elemental exchange. In: Proceedings of the 29th Lunar and Planetary Science Conference.

Drake, M.J., 2000. Accretion end primary differentiation of the earth: a personal journey. Geochim. Cosmochim. Acta 64, 2363–2370.

Dreibus, G., Palme, H., 1996. Cosmochemical constraints on the sulfur content in the earth's core. Geochim. Cosmochim. Acta 60, 1125–1130.

Fei, Y., Mao, H.-K., Mysen, B., 1991. Experimental determination of element partitioning and calculation of phase relation in the MgO–FeO–SiO_2 system at high pressure and high temperature. J. Geophys. Res. 96, 2157–2169.

Fleet, M.E., Mac Rae, N.D., 1987. Sulfidation of Mg-rich olivine and the stability of niningerite in enstatite chondrites. Geochim. Cosmochim. Acta 51, 1511–1521.

Fogel, R.A., 1998. High sulfur-low iron silicate melts: low oxygen fugacity phenomena of importance to aubrite formation. In: Proceedings of the 61st Annual Meteoritical Society Meeting.

Frost, D.J., Langhenhorst, F., Van Aken, P.A., 2001. Fe–Mg partitioning between ringwoodite and magnesiowüstite and the effect of pressure, temperature, and oxygen fugacity. Phys. Chem. Miner. 26, 455–470.

Frost, D.J., 2003. Fe^{2+}–Mg partitioning between garnet, magnesiowüstite, and (Mg, Fe)SiO_4 phases of the transition zone. Am. Min. 88, 387–397.

Gessmann, C.K., Rubie, D.C., McCammon, C.A., 1999. Oxygen fugacity dependence of Ni, Co, Mn, Cr, V and Si partitioning between liquid metal and magnesiowustite at 9–18 GPa and 2200 °C. Geochim. Cosmochim. Acta 63, 1853–1863.

Gessmann, C.K., Wood, B.J., Rubie, D.C., Kilburn, M.R., 2001. Solubility of silicon in liquid metal at high pressure: implications for the composition of the earth's core. Earth Planet. Sci. Lett. 184, 367–376.

Gillet, P., Le Cleach, A., Madon, M., 1990. High temperature Raman spectroscopy of SiO_2 and GeO_2 polymorphs. Anharmonicity and thermodynamic properties at high temperatures. J. Geophys. Res. 81, 21635–21655.

Guyot, F., Zhang, J., Martinez, I., Matas, J., Ricard, Y., Javoy, M., 1997. P–V–T measurements of iron silicide (ε-FeSi). Implications for silicate–metal interactions in the early earth. Eur. J. Mineral. 9, 277–285.

Holzheid, A., Grove, T.L., 2002. Sulfur saturation limits in silicate melts and their implications for core formation scenarios for terrestrial planets. Am. Min. 87, 227–237.

Ito, E., Morooka, K., Ujike, O., Katsura, T., 1995. Reaction between molten iron and silicate melts at high pressure: implications for the chemical evolution of the earth's core. J. Geophys. Res. 100, 5901–5910.

Javoy, M., 1995. The integral enstatite chondrite model of the earth. Geophys. Res. Lett. 22, 2219–2222.

Karato, S., Murthy, V.R., 1997. Core formation and chemical equilibrium in the earth. I. Physical considerations. Earth Planet. Sci. Lett. 100, 61–79.

Keil, K., 1989. Enstatite meteorites and their parents bodies. Meteoritics 24, 195–208.

Kilburn, M.R., Wood, B.J., 1997. Metal–silicate partitioning and the incompatibility of S and Si during core formation. Earth Planet. Sci. Lett. 152, 139–148.

Larimer, J.W., Bartholomay, M., 1979. The role of carbon and oxygen in cosmic gases: some applications to the chemistry and mineralogy of enstatite chondrites. Geochim. Cosmochim. Acta 43, 1455–1466.

Larimer, J.W., Ganaparthy, R., 1987. The trace element chemistry of CaS in enstatite chondrites and some implications regarding its origin. Earth Planet. Sci. Lett. 84, 123–134.

Li, J., Agee, C.B., 1996. Geochemistry of mantle-core differentiation at high pressure. Nature 381, 686–689.

Li, J., Agee, C.B., 2001a. Element partitioning constraints on the light element composition of the earth's core. Geophys. Res. Lett. 28, 81–84.

Li, J., Agee, C.B., 2001b. The effect of pressure, temperature, oxygen fugacity and composition of nickel and cobalt between liquid Fe–Ni–S alloy and liquid silicate: implications for the earth's core formation. Geochim. Cosmochim. Acta 65, 1821–1832.

Liu, M., Fleet, M.E., 2001. Partitioning of siderophile elements (W, Mo, As, Ag, Ge, Ga, and Sn) and Si in the Fe–S system and their fractionation in iron meteorites. Geochim. Cosmochim. Acta 65, 671–682.

MacDonald, G.J.F., Knopoff, L., 1958. On the chemical composition of the outer core. J. Geophys. Res., Astron. Soc. 1, 284–297.

Malavergne, V., Siebert, J., Guyot, F., Gautron, L., Combes, R., Hammouda, T., Borenstajn, S., Frost, D.J., Martinez, I., 2004. Si in the core? New high pressures and high temperature experimental data. Geochim. Cosmochim. Acta, submitted for publication.

McCoy, T.J., Dickinson, T.L., Lofgren, G.E., 1999. Partial melting of the indarch (EH4) meteorite: a textural view of melting and melt migration. Meteorit. Planet. Sci. 34, 735–746.

Murthy, V.R., Hall, H.T., 1970. The origin and chemical composition of the earth's core. Phys. Earth Planet. Inter. 2, 276–282.

Murthy, V.R., 1991. Early differentiation of the earth and the problem of mantle siderophile elements: a new approach. Science 253, 303–306.

O'Neill, H.St.C., Canil, D., Rubie, D.C., 1998. Oxide-metal equilibria to 2500 °C and 25 GPa: implications for core formation and the light component in the earth's core. J. Geophys. Res. 103, 12239–12260.

Othani, E., Yurimoto, H., Seto, S., 1997. Element partitioning between metallic liquid, silicate liquid, and lower-mantle minerals: implications for core formation of the earth. Phys. Earth Planet. Inter. 100, 97–114.

Peiris, M.S., Campbell, A.J., Heinz, D.L., 1994. Compression of MgS to 54 GPa. J. Phys. Chem. Solids 1994, 419–431.

Poirier, J.P., 1994. Light elements in the earth's outer core: a critical review. Phys. Earth Planet. Inter. 85, 319–337.

Raghavan, V., 1988. Phase Diagrams of Ternary Iron Alloys. Part 2. Ternary Systems Containing Iron and Sulphur. The Indian Institute of Metals, Calcutta.

Rauch, M., Keppler, H., Hafner, W., Poe, B., Wokan, A., 1996. A pressure-induced phase transition in $MgSiO_3$-rich garnet revealed by Raman spectroscopy. Am. Min. 81, 1289–1292.

Righter, K., Drake, M.J., Yaxley, G., 1997. Prediction of siderophile element metal–silicate partition coefficient to 20 GPa and 2800 °C: the effect of pressure, temperature, fO_2 and silicate and metallic melt composition. Phys. Earth Planet. Inter. 100, 115–134.

Ringwood, A.E., Hibberson, W., 1991. Solubilities of mantle oxides in molten iron at high pressures and temperatures: implications for the composition and formation of earth's core. Earth Planet. Sci. Lett. 102, 235–251.

Rubie, D.C., 1999. Characterising the sample environment in multianvil high-pressure experiments. Phase Trans. 68, 431–451.

Sanloup, C., Fei, Y., 2004. Closure of the Fe–S–Si in liquid miscibility gap at high pressure and its implications for planetary core formation. In: Proceedings of the 35th Lunar and Planetary Science Conference. Phys. Earth planet Inter., submitted for publication.

Thiéblaut, L., Téqui, C., Richet, P., 1999. High-temperature heat capacity of grossular ($Ca_3Al_2Si_3O_{12}$), enstatite ($MgSiO_3$), and titanite ($CaTiSiO_3$). Am. Min. 84, 848–855.

Tronnes, R.G., 2000. Melting relations and major element partitioning in an oxidized bulk earth model at 15–26 GPa. Lithos 53, 233–245.

Wade, J., Wood, B.J., 2001. The earth's 'missing' niobium may be in the core. Nature 409, 75–78.

Walker, D., Norby, L., Jones, J.H., 1993. Superheating effects on metal/silicate partitioning of siderophile elements. Science 262, 1858–1861.

Walter, M.J., Newsom, H., Ertel, W., Holzeid, A., 2000. Siderophile elements in the earth and moon: metal–silicate partitioning and implications for core formation. In: Canup, R.M., Righter, K. (Eds.), Origin of the Earth and Moon. University of Arizona, Tucson.

Wänke, H., Dreibus, G., 1988. Chemical composition and accretion history of terrestrial planets. Phil. Trans. Roy. Soc. Lond. A 325, 545–557.

Wood, B.J., 2000. Phase transformations and partitioning relations in peridotite under lower mantle conditions. Earth Planet. Sci. Lett. 174, 341–354.